Molecular Simulation of Henry's Constant at Vapor−Liquid and Liquid−Liquid Phase Boundaries

Richard J. Sadus

Computer Simulation and Physical Applications Group, School of Computer Science and Software Engineering, Swinburne University of Technology, P.O. Box 218, Hawthorn, Victoria 3122, Australia

Received: November 13, 1996; In Final Form: February 26, 1997[⊗]

The Gibbs ensemble is implemented to determine Henry's constant from the residual chemical potential at infinite dilution at the vapor−liquid and liquid−liquid phase boundaries. Results are reported for 12 different single solvent + solute systems at several temperatures between the triple point and critical point of the solvent. The effect of solvent polarity and different solvent−solute dispersion interactions are investigated. Solvent−solute and solvent−solvent interactions are represented by either Lennard-Jones or Keesom intermolecular potentials. The temperature at which the residual chemical potential at infinite dilution equals zero is estimated. Simulations are also reported for three different mixed solvent + solute systems at conditions for liquid−liquid coexistence.

1. Introduction

Henry's constant is a well-known measure of a solute's solubility in a particular solvent; i.e., the solubility of a molecule is inversely proportional to Henry's constant. Extensive compilations of experimental Henry's constant are available[1] for many solutes in different solvents. Henry's constant is also a potentially useful measure of the strength of unlike solvent−solute interactions because it is obtained at infinite dilution.

Henry's constant (H) can be related directly to the residual chemical potential at infinite dilution of the solute[2] (c_r^∞):

$$H = \rho kT \exp\left\langle \frac{c_r^\infty}{kT} \right\rangle \tag{1}$$

where the angled brackets represent an ensemble average, k is the Boltzmann constant, T is temperature and ρ is the density of the solvent. Equation 1 permits the calculation of Henry's constant from molecular simulation by employing a Widom[3] test particle approach. During a simulation, a test particle representing the solute is inserted randomly into the solvent and the interactions between the solute test particle and all the solvent molecules are evaluated. The residual chemical potential at infinite dilution, or Henry's constant obtained from this procedure, is solely attributable to unlike solvent−solute interactions. The composition of the solute in the solvent is exactly zero, as required for infinite dilution because the test particle is a "ghost" that does not affect the equilibrium. Shing et al.[2,4] reported simulations of Henry's constant for the Lennard-Jones potential with various values of intermolecular parameters. Simulation methods have also been developed for calculating Henry's constant for chain molecules,[5] and several simulation studies of solubility at supercritical conditions have been reported.[6−11]

Previous simulation studies[2, 4−11] have only reported values of Henry's constant at conditions away from the phase boundary. In this work, the Gibbs ensemble[12,13] was implemented to determine Henry's constant at conditions corresponding to either vapor−liquid or liquid−liquid phase coexistence. Results are reported for single-solvent and mixed-solvent systems containing both nonpolar and dipolar molecules.

2. Theory

2.1. Intermolecular Potentials. The interactions between different solvent molecules or solvent and solute molecules were calculated using a "Lennard-Jones + dipole term" potential; i.e.,

$$v(r) = 4\epsilon\left[\left(\frac{\sigma}{r_{ij}}\right)^{12} - \left(\frac{\sigma}{r_{ij}}\right)^{6}\right] + \phi_{\text{dipole}} \tag{2}$$

Equation 2 contains the nonpolar contributions to the characteristic depth (ϵ) and collision diameter (σ) for the Lennard-Jones potential[14] plus a Boltzmann average for the contribution from dipole interactions[15]

$$\phi_{\text{dipole}} = -\frac{\mu_i^2 \mu_j^2}{3kTr_{ij}^6} \tag{3}$$

The Boltzmann average is not valid for strong dipoles that exert a long-range influence. However, the simplicity of the Lennard-Jones + Keesom potential, hereafter referred to as the Keesom potential, is advantageous for phase equilibria simulations. Recent work[16,17] indicates that the Keesom potential is valid for weak dipoles ($(\mu^*)^2 \leq 1$).

2.2. Simulation Details. The NVT−Gibbs ensemble[12] was used to simulate the coexistence of liquid and vapor phases of a single pure solvent, whereas NPT−Gibbs ensemble[13] calculations were performed for mixed-solvent binary mixtures. A total of 300 molecules were partitioned between 2 boxes to simulate the vapor and liquid phases or two liquid phases. The temperature of the entire system was held constant, and surface effects were avoided by placing each box at the center of a periodic array of identical boxes. Equilibrium was achieved by attempting molecular displacements (for internal equilibrium), volume fluctuations (for mechanical equilibrium), and particle interchanges between the boxes (for material equilibrium).

The simulations were performed in cycles with each cycle typically consisting of 300 attempted displacements, a single volume fluctuation, and typically 100−500 interchange attempts. The maximum molecular displacement and volume changes were adjusted to obtain, where possible, a 50% acceptance rate for the attempted move. Ensemble averages were accumulated only after the system had reached equilibrium. The equilibration period was 5000−10000 cycles, and a further 5000−10000 cycles were used to accumulate the averages. The calculations were truncated at intermolecular separations greater than half the box length, and appropriate long-range corrections[19] were used to obtain the full contribution of pair interactions to energy

[⊗] Abstract published in *Advance ACS Abstracts,* April 15, 1997.

S1089-5647(96)03793-5 CCC: $14.00

TABLE 1: Intermolecular Potential Parameters for Single Solvent (Component 1) + Solute (Component 2) Systems

system	ϵ_{11}*	ϵ_{22}*	ϵ_{12}*	σ_{11}*	σ_{22}*	σ_{12}*	$(\mu_{11}^*)^2$	$(\mu_{22}^*)^2$
I	1	0.5	0.7071	1	1	1	0	0
II	1	0.95	0.9747	1	1	1	0	0
III	1	1.5	1.2247	1	1	1	0	0
IV	1	1	1	1	0.5	0.75	0	0
V	1	1	1	1	0.95	0.975	0	0
VI	1	1	1	1	0.25	0.625	0	0
VII	1	0.5	0.7071	1	1	1	1	0
VIII	1	0.95	0.9747	1	1	1	1	0
IX	1	1.5	1.2247	1	1	1	1	0
X	1	1	1	1	0.5	0.75	1	0
XI	1	1	1	1	0.95	0.975	1	0
XII	1	1	1	1	0.25	0.625	1	0

and pressure. A typical run required 1−2 CPU h on a Cray YMP-EL computer.

After equilibrium was obtained, a "ghost" test particle representing the solute was inserted randomly into the liquid phase during each particle interchange attempt. The residual chemical potential at infinite dilution was calculated from the formula proposed by Smit and Frenkel[18]

$$c_r^\infty = -kT \ln\left[\frac{\left\langle V \exp\left(-\frac{E}{kT}\right)\right\rangle}{\langle V\rangle}\right] \tag{4}$$

where V is the volume of the solvent and E is the energy resulting from the interaction of the solute molecule with all the molecules of the solvent. For the Gibbs ensemble, eq 4 is more accurate than the Widom[3] alternative at temperatures near the critical point. The interchange step proceeded normally following this ghost insertion.

3. Results and Discussion

3.1. Single Solvent + Solute Systems at Conditions for Vapor−Liquid Coexistence. The parameters characteristic of various solvent−solute interactions are summarized in Table 1. The unlike interaction parameters for systems I−XII were obtained by combining different interaction parameters for the pure solvent (i) and pure solute (j) molecules

$$\epsilon_{ij}^* = \sqrt{\epsilon_{ii}^* \epsilon_{jj}^*} \tag{5}$$

$$\sigma_{ij}^* = \frac{\sigma_{ii}^* + \sigma_{jj}^*}{2} \tag{6}$$

Again, it should be noted that only the unlike solvent−solute interactions contribute to the residual chemical potential at infinite dilution because $x_j = 0$. In eqs 5 and 6, the * denotes that the intermolecular parameters are reduced with respect to the corresponding parameter of component 1.

Three distinct categories of solvent−solute interactions were studied. Systems I−III represent solvent−solute interactions with identical σ parameters but with varying ϵ values. Systems IV−VI examine components with identical ϵ values, whereas the σ parameters are different. The effect of a dipolar solvent on a nonpolar solute is investigated for systems VII−XII. Either the ϵ parameters (systems VII−IX) or the σ parameters (systems X−XII) were allowed to vary in these systems. The residual chemical potentials at infinite dilution for different vapor−liquid phase coexistence conditions are summarized in Tables 2 and 3. The normal convention was adopted for the reduced density ($\rho^* = \rho\sigma^3$), temperature ($T^* = kT/\epsilon$), pressure ($P^* = P\sigma^3/\epsilon$), dipole moment ($(\mu^*)^2 = \mu^2/\epsilon\sigma^3$), and residual chemical potential at infinite dilution ($c_r^{\infty *} = c_r^\infty/\epsilon$).

TABLE 2: Residual Chemical Potentials at Infinite Dilution at the Vapor−Liquid Coexistence Point for Nonpolar Systems with Different σ and ϵ Solvent−Solute Interaction Parameters[a]

			$c_r^{\infty *}$					
T*	P*	ρ*	I	II	III	IV	V	VI
0.8	0.005(2)	0.802(5)	−0.407	−3.217	−5.982	−2.792	−3.500	−1.858
0.9	0.012(4)	0.753(6)	−0.537	−3.216	−5.824	−2.519	−3.376	−2.088
1.0	0.024(6)	0.701(6)	−0.675	−3.170	−5.615	−2.246	−3.272	−1.641
1.1	0.046(14)	0.637(10)	−0.706	−2.929	−5.120	−1.984	−3.009	−1.413
1.2	0.075(21)	0.559(20)	−0.742	−2.658	−4.572	−1.683	−2.710	−1.179
1.25	0.121(26)	0.521(11)	−0.679	−2.450	−4.229	−1.548	−2.494	−1.078

[a] The values in parentheses represent the uncertainty in the last digit. The uncertainty in $c_r^{\infty *}$ is typically ±0.05.

TABLE 3: Residual Chemical Potentials at Infinite Dilution at the Vapor−Liquid Coexistence Point of Dipolar Solvent Systems with Different σ and ϵ Solvent−Solute Interaction Parameters[a]

			$c_r^{\infty *}$					
T*	P*	ρ*	VII	VIII	IX	X	XI	XII
1.0	0.013(4)	0.808(5)	0.452	−2.523	−5.532	−2.238	−2.619	−1.801
1.1	0.029(5)	0.759(6)	0.709	−2.068	−4.557	−2.038	−2.353	−1.596
1.2	0.046(10)	0.697(7)	0.199	−2.161	−4.490	−1.818	−2.325	−1.408
1.3	0.077(15)	0.636(7)	0.114	−1.994	−4.073	−1.605	−2.139	−1.207
1.35	0.088(34)	0.578(15)	−0.241	−1.862	−4.076	−1.482	−2.249	−1.085

[a] The values in parentheses represent the uncertainty in the last digit. The uncertainty in $c_r^{\infty *}$ is typically ±0.05.

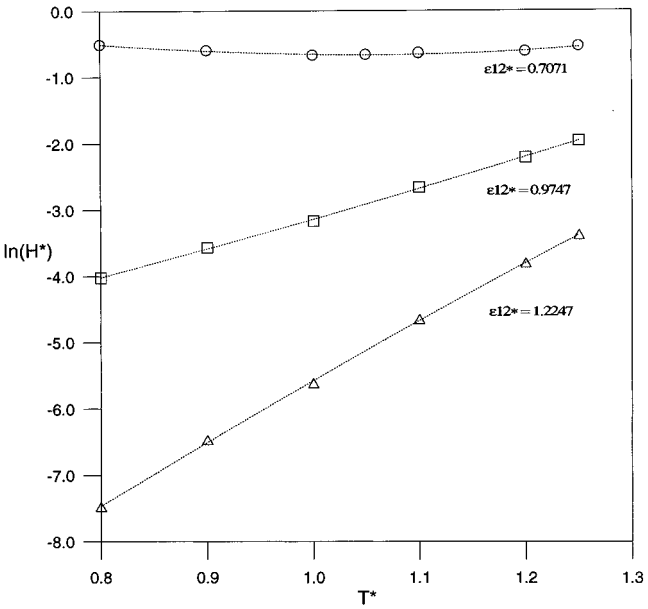

Figure 1. Effect of ϵ_{12}* on Henry's constant at different temperatures on the vapor−liquid boundary for systems I (○), II (□), and III (△).

The calculations for the Lennard-Jones solvent (Table 2) cover almost the entire range of vapor−liquid coexistence from the triple point ($T^* \approx 0.75$) to the critical point ($T^{*c} = 1.316$).[20] It is apparent from Table 2 that $c_r^{\infty *}$ generally increases with increasing temperature and decreasing density. In contrast, a decrease in $c_r^{\infty *}$ is observed initially as the temperature of system I increases. The interaction between the solvent and solute for this system is particularly weak ($\epsilon_{12}^* = 0.7071$) compared with the strength of unlike interactions for the other systems (Table 1).

Figure 1 illustrates the variation of the reduced Henry's constant ($H^* = H/\rho kT$) with temperature for systems I−III. These systems are distinguishable solely by their different solvent−solute ϵ_{12}* parameters. It is apparent from Figure 1

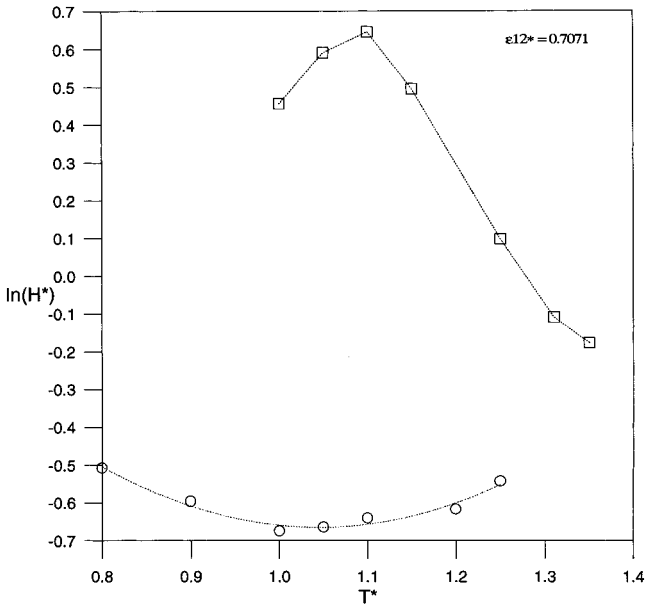

Figure 2. Comparison of Henry's constant in a nonpolar solvent (○, system I) and dipolar (□, system VII) solvents at different temperatures on the vapor−liquid phase boundary.

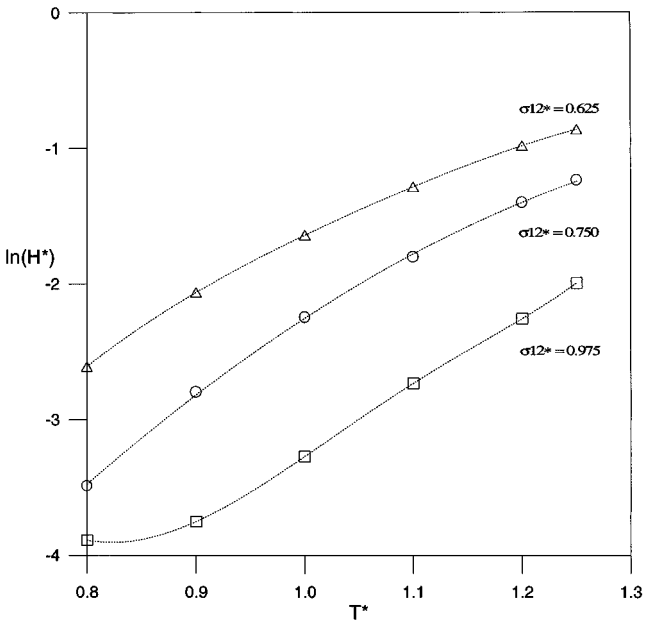

Figure 3. Effect of σ_{12}* on Henry's constant at different temperatures on the vapor−liquid phase boundary for systems IV (○), V (□), and VI (△).

that there are large differences in H* for the different solutes at low temperatures. However, the differences in H* diminish rapidly as the critical point of the solvent is approached. For both systems II and III, there is a progressive increase in H* with increasing temperature. In contrast, the values of H* for system I pass through a minimum near $T^* = 1$. This is illustrated in greater detail in Figure 2.

The effect of varying the solvent−solute σ_{12}* parameter on H* is illustrated in Figure 3 for systems IV−VI. For all of these systems, there is a large difference in H* at conditions close to the triple point. This disparity in H* decreases rapidly with increasing temperature. Comparing the results for systems IV−VI indicates that a reduction in σ_{12}* can reduce significantly the value of H*. Consequently, solubility is enhanced if the solute and solvent molecules are of similar size.

The residual chemical potentials at infinite dilution of solutes in a dipolar solvent are summarized in Table 3. Results are

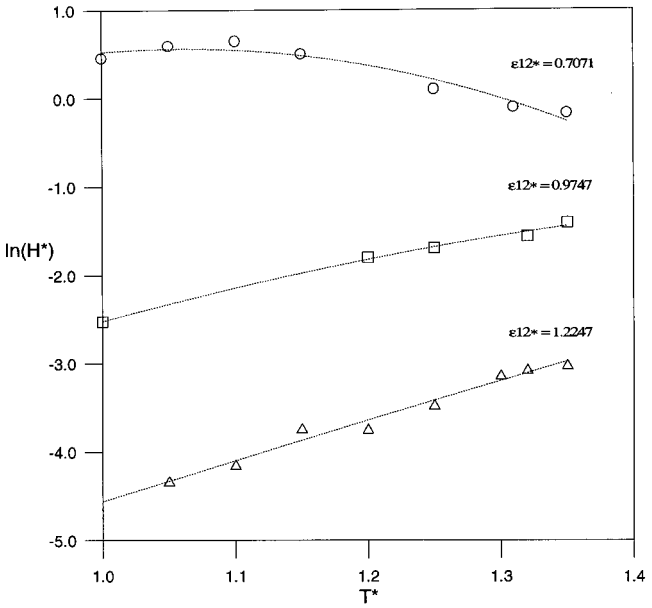

Figure 4. Effect of a dipolar solvent on Henry's constant at different temperatures on the vapor−liquid phase boundary for systems VII (○), VIII (□), and IX (△).

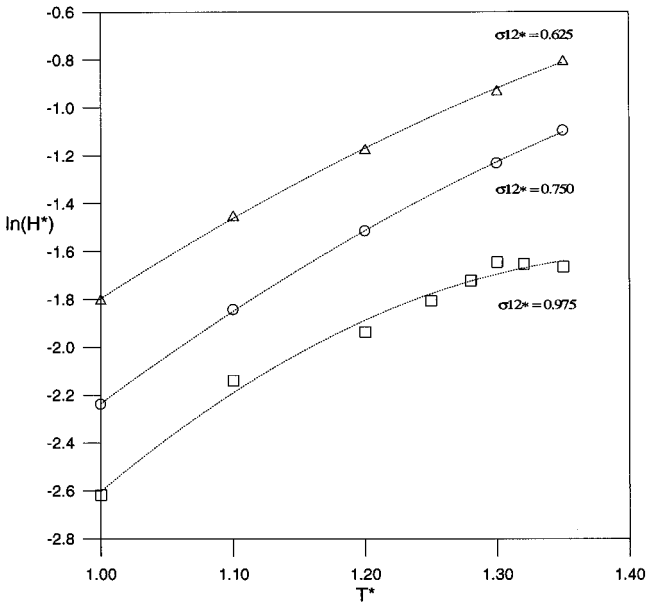

Figure 5. Effect of a dipolar solvent on Henry's constant at different temperatures on the vapor−liquid phase boundary for systems X (○), XI (□), and XII (△).

included in the vicinity of the solvent's critical point which has been reported previously[16] at $T^{*c} = 1.43$. It is apparent that c_r^{∞}* generally increases with increasing temperature and decreasing density.

The effect of a dipolar solvent on the value of H* is illustrated in Figure 4 for systems VII−IX which have identical ϵ_{12}* values to systems I−III. The values of H* for systems VIII ($\epsilon_{12}^* = 0.9747$) and IX ($\epsilon_{12}^* = 1.2247$) have the same temperature behavior as their counterparts (systems II and III in Figure 1) in a nonpolar solvent. However, comparison of Figure 4 with Figure 1 indicates that the effect of the dipole at any given temperature is to increase H* substantially. Consequently, the nonpolar solute is less soluble in the dipolar solvent compared with the nonpolar solvent. In contrast to the other systems, the H* behavior of system VII ($\epsilon_{12}^* = 0.7071$) passes through a maximum. This behavior is illustrated in greater detail in Figure 2.

TABLE 4: Estimated Values of Reduced Temperature at Which $c_r^{\infty *} = 0$

system	T^*_0	system	T^*_0
I	1.49	VI	1.65
II	1.69	VIII	1.91
III	1.64	IX	1.99
IV	1.65	X	1.86
V	1.65	XII	1.75

TABLE 5: Intermolecular Potential Parameters for Mixed-Solvent (Component 1 and Component 2) + Solute (Component 3) Systems, $(\mu^*)^2 = 0$ for All Components

system	ϵ_{11}^*	ϵ_{22}^*	ϵ_{33}^*	ϵ_{12}^*	ϵ_{13}^*	ϵ_{23}^*	σ_{11}^*	σ_{22}^*	σ_{33}^*	σ_{12}^*	σ_{13}^*	σ_{23}^*
XIII	1	0.75	1	0.606	1	0.866	1	0.95	1	0.975	1	0.975
XIV	1	0.75	1	0.606	0	0.866	1	0.95	1	0.975	1	0.975
XV	1	0.75	1	0.606	1	0	1	0.95	1	0.975	1	0.975

It is of interest to compare system VII with system I (Figure 2). The Lennard-Jones parameters for solvent−solute interactions are identical, and the systems are distinguishable solely by the polarity of the solvent. In a nonpolar solvent, Henry's constant attains a minimum value, whereas a maximum value is reached in the dipolar solvent. The Lennard-Jones energy interaction parameter for mixtures I and VII is relatively weak. In the absence of strong unlike dispersion interactions, a weak dipole can have a substantial effect on solubility.

Figure 5 illustrates the temperature variations of systems X−XII which are the dipolar analogues of systems IV−VI. It is apparent that decreasing σ_{12}^* results in an increase in H^*. A disparity in size between the solute and dipolar solvent molecule will result in a reduction in solubility. The values of H^* in the dipolar solvent are also substantially larger than for the nonpolar case (Figure 3).

From a molecular perspective, the progressive increase in $c_r^{\infty *}$ (and therefore H^*) with increasing temperature can be rationalized in terms of the increasing dominance of repulsive interactions at high temperatures. Therefore, it is useful to determine the value of T^* at which $c_r^{\infty *} = 0$, i.e., the temperature at which intermolecular repulsions dominate completely. The values of temperatures at this condition (denoted T^*_0) could be a useful indicator of the strength of solvent−solute interaction and solubility. High values of T^*_0 for a particular solvent indicate strong solvent−solute interactions whereas weak interaction is reflected by low values.

Values of T^*_0 can be estimated by extrapolating the simulation data into the supercritical phase (Table 4). The values of T^*_0 should be regarded only as approximate estimates because of the inexact nature of the extrapolation. Generally, T^*_0 increases with increasing strength of solvent−solute interactions (ϵ_{12}^*). The values of T^*_0 for the dipolar solvent are higher than for the nonpolar solvent, reflecting the phase shift caused by dipolar solvent−solvent interactions. The σ_{12}^* parameter has no noticeable effect on the value T^*_0 for the nonpolar solvents (systems IV−VI). The value of T^*_0 is sensitive to the σ_{12}^* parameter for the dipolar solvents (systems X−XII). The values of T^*_0 for systems VII and XI are not given in Table 4 because the data for these systems could not be extrapolated reliably.

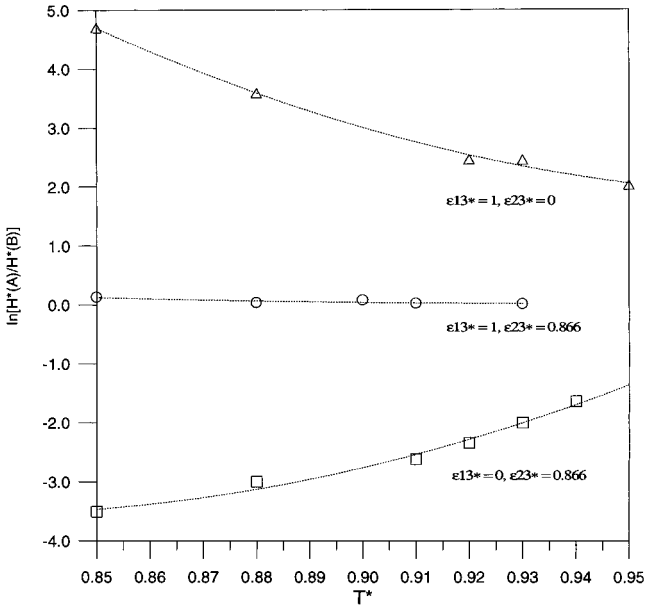

Figure 6. Difference in Henry's constant between phase A and B at different temperatures on the liquid−liquid phase boundary for systems XIII (○), XIV (□), and XV (△).

3.2. Mixed Solvent + Solute Systems at Conditions for Liquid−Liquid Coexistence. Molecular simulation enables us to examine the solubility in a mixed solvent which poses considerably more experimental and theoretical difficulties when compared with the single solvent + solute case. Indeed, experimental Henry's constant data for mixed solvents are relatively scarce. To simulate liquid−liquid equilibria, we chose values of the solvent−solvent interaction parameters (ϵ_{12}^* and σ_{12}^*) and a pressure ($P^* = 0.125$) which were known[17,21] to result in liquid−liquid phase separation. Earlier calculations[17] established a liquid−liquid critical point at $T^{*c} = 0.956$ for this combination of solvent molecules. Arbitrary values for the solvent−solute interactions (ϵ_{13}^*, ϵ_{23}^*, σ_{13}^*, and σ_{23}^*) were used. The interaction parameters for systems XIII−XV are summarized in Table 5.

The residual chemical potentials at infinite dilution of solutes in both solvent liquid phases are summarized in Table 6. The less dense phase is denoted by A, whereas the more dense phase is denoted by B. In contrast to the case of a single solvent + solute, $c_r^{\infty *}$ values for the mixed solvent + solute systems are the result of two different solvent−solute interactions. The values of $c_r^{\infty *}$ generally increase with increasing temperature and decreasing density. For system XIII, $c_r^{\infty *}$ is similar in both phases, whereas there are large differences in the values of $c_r^{\infty *}$ in the two phases for systems XIV and XV.

The difference in H^* between phases A and B at different temperatures is illustrated in Figure 6. The σ_{13}^* and σ_{23}^*

TABLE 6: Residual Chemical Potentials at Infinite Dilution at the Liquid−Liquid Coexistence Point of a Mixed Solvent[a]

	phase A					phase B				
			$c_r^{\infty *}$					$c_r^{\infty *}$		
T^*	x_1	ρ^*	XIII	XIV	XV	x_1	ρ^*	XIII	XIV	XV
0.85	0.064(15)	0.729(18)	−3.312	−3.436	−0.513	0.924(13)	0.776(5)	−3.407	−0.453	−4.508
0.88	0.150(20)	0.650(18)	−3.228	−3.093	−1.028	0.921(16)	0.763(8)	−3.310	−0.453	−4.183
0.91	0.181(33)	0.610(24)	−3.270	−2.874	−1.157	0.913(21)	0.742(9)	−3.245	−0.491	−3.998
0.93	0.285(50)	0.572(30)	−3.259	−2.472	−1.649	0.886(18)	0.732(9)	−3.270	−0.608	−3.924
0.94	0.206(36)	0.533(43)	−3.039	−2.610	−1.063	0.853(31)	0.711(17)	−3.293	−1.069	−3.821

[a] The values in parentheses represent the uncertainty in the last digit. The uncertainty in $c_r^{\infty *}$ is typically ±0.05.

parameters for systems XIII−XV are identical, whereas each system has different ϵ_{13}* and ϵ_{23}* parameters. There is very little difference in H* for system XIII, and the solute is almost equally soluble in either solvent phase. However, when ϵ_{13}* = 0, the solute is much more soluble in phase A compared with phase B. Conversely, when ϵ_{23}* = 0, the solute exhibits a preference for phase B at the expense of phase A.

4. Conclusions

Molecular simulation data for the residual chemical potential at infinite dilution (Henry's constant) quantify the effect of intermolecular interactions on solubility. The magnitude of the ϵ_{ij}* parameters and the polarity of the solvent are the dominant influences on solubility. If the contribution to ϵ_{ij}* of unlike dispersion interactions is relatively small, the reduced Henry's constant for a solute in a nonpolar solvent passes through a minimum value. In contrast, if the solvent is dipolar and the unlike dispersion interactions are weak, the reduced Henry's constant can attain a maximum value. Consequently, the polarity of the solvent is likely to have an important influence on solubility when solvent−solute dispersion interactions are weak. Variations in σ_{ij}* generally have a lesser role. Henry's constant increases with increasing size difference between the solute and solvent. The temperature at which the residual infinite dilution chemical potential is equal to zero can be used as an indicator of solubility in a particular solvent.

Acknowledgment. The simulations were performed on the Swinburne University of Technology Cray YMP-EL and the Australian National University Supercomputing Centre Fujitsu computers.

References and Notes

(1) See, for example: Young, C. L. *Solub. Data Ser.* **1981**, 8.

(2) Shing, K. S.; Gubbins, K. E.; Lucas, K. *Molec. Phys.* **1988**, *65*, 1235.

(3) Widom, B. *J. Chem. Phys.* **1963**, *39*, 2808.

(4) Shing, K. S.; Gubbins, K. E. *Molec. Phys.* **1983**, *49*, 1121.

(5) de Pablo, J. J.; Laso, M.; Suter, U. W. *Macromolecules* **1993**, *26*, 6180.

(6) Shing, K. S.; Chung, S. T. *J. Phys. Chem.* **1987**, *91*, 1674.

(7) Nouacer, M.; Shing, K. S. *Molec. Sim.* **1989**, *2*, 55.

(8) Eya, H.; Iwai, Y.; Fukuda, T.; Arai, Y. *Fluid Phase Equilib.* **1992**, *77*, 39.

(9) Iwai, Y.; Mori, Y.; Koga, Y.; Arai, Y.; Eya, H. *J. Chem. Eng. Jpn.* **1994**, *27*, 334.

(10) Iwai, Y.; Koga, Y.; Hata, Y.; Uchida, H.; Arai, Y. *Fluid Phase Equilib.* **1995,** *104*, 403.

(11) Iwai, Y.; Uchida, H.; Koga, Y.; Mori, Y.; Arai, Y. *Fluid Phase Equilib.* **1995**, *111*, 1.

(12) Panagiotopoulos, A. Z. *Molec. Phys.* **1987**, *61*, 813.

(13) Panagiotopoulos, A. Z.; Quirke, N.; Stapleton, M.; Tildesley, D. J. *Molec. Phys.* **1988**, *63*, 527.

(14) Maitland, G. C.; Rigby, M.; Smith, E. B.; Wakeham, W. A. *Intermolecular Forces: Their Origin and Determination*; Clarendon: Oxford, 1981; pp 28−30.

(15) Reed, T. M.; Gubbins, K. E. *Applied Statistical Mechanics: Thermodynamic and Transport Properties of Fluids*; McGraw-Hill: New York, 1973; pp 157−161.

(16) Sadus, R. J. *Molec. Phys.* **1996**, *87*, 879.

(17) Sadus, R. J. *Molec. Phys.* **1996,** *89*, 1187.

(18) Smit, B.; Frenkel, D. *Molec. Phys.* **1989**, *68*, 951.

(19) Allen, M. P.; Tildesley, D. J. *Computer Simulation of Liquids*; Clarendon: Oxford, 1989; pp 155−164.

(20) Gubbins, K. E. in *Models for Thermodynamic and Phase Equilibria Calculations*; Sandler, S. I., Ed.; Marcel Dekker: New York, 1994; p 554.

(21) Guo, M. X.; Li, Y. G.; Li, Z. C.; Lu, J. F. *Fluid Phase Equilib.* **1994**, *98*, 129.